PERGAMON

Quaternary Science Reviews 21 (2002) 343–360

QSR

Into and out of the Last Glacial Maximum: sea-level change during Oxygen Isotope Stages 3 and 2

Kurt Lambeck[a,*], Yusuke Yokoyama[b,c], Tony Purcell[a]

[a] *Research School of Earth Sciences, Australian National University, Canberra, ACT 0200, Australia*
[b] *Space Sciences Laboratory, University of California, Berkeley, CA, USA*
[c] *Lawrence Livermore National Laboratory, Livermore, CA, USA*

Received 11 January 2001; accepted 18 May 2001

Abstract

Sea-level data from seven different regions have been used to estimate the global change in ocean and ice volumes for the time interval leading into and out of the Last Glacial Maximum (LGM). The estimates are earth-model dependent and parameters are chosen that minimize discrepancies between the individual estimates for each region. Good coherence between estimates from different localities has been found. The main conclusions are: (i) Ice volumes approached their maximum values 30 000 (calendar) years ago and remained nearly constant until 19 000 years ago. This defines the period of maximum global glaciation. (ii) The post-LGM sea-level rise is marked by changes in rates with maximum rates of about 15 mm/year occurring from 16,000 to 12,500 years ago and again from 11,500 to 9000 years ago. Ice volumes in the interval between these two periods of rapid rise, corresponding to the Younger Dryas, is nearly constant. (iii) The melting at the end of the LGM is characterized by an initially high rate over about 500 years followed by about 2500 years of a comparatively slow increase in ocean volume. (iv) The lead into the LGM is characterized by a sea-level fall of about 50 m occurring within a few thousand years. Similar rates of falling and rising sea levels occur during the earlier part of the oxygen isotope stage 3 interval.

1. Introduction

During the Last Glacial Maximum (LGM) large ice sheets covered high latitude Europe and North America and the Antarctic ice sheet was more extensive than today. Sea levels stood some 120–130 m lower than today. The Earth's climate at this time was also distinctly different from that of the present interglacial conditions. The sea-level changes are indicators of growth and decay of ice sheets and provide, thereby, boundary conditions on models of climate change. Aspects of the sea-level change that are particularly relevant to understanding climate change and the response of the ice sheets to this change are (i) the timing of the onset and termination of the low stands that mark the LGM and (ii) the determination of the rates of sea-level rise or fall leading into and out of the LGM.

Sea-level change caused by the growth or decay of ice sheets is spatially variable because of the adjustment of the earth's surface to the time-dependent ice-water load and because of the changing gravitational potential of the earth-ocean-ice system. Observations of relative sea-level change, therefore, do not bear a simple relation to changes in ice volume, (or ice-equivalent sea level) and at most localities corrections for glacio-hydro-isostasy will be required. Even sea levels at ocean island sites are not immune from isostatic effects. Only in some special instances, where the separate isostatic responses to the changing water and ice loads fortuitously cancel out, will the relationship be relatively straight forward. Thus, in general, changes in ocean volume inferred from sea level data will be dependent on the models of glacio-hydro-isostasy and be functions of the spatial and temporal distribution of the ice load and of the rheological response of the Earth to surface loading. However, through an iterative approach, useful estimates of grounded and land-based ice volumes can be inferred from sea-level information, particularly when the data are from sites that lie far from the former ice

*Corresponding author. Tel.: +61-2-6249-5161; fax: +61-2-6249-5443.
E-mail address: kurt.lambeck@anu.edu.au (K. Lambeck).

0277-3791/02/$ - see front matter
PII: S0277-3791(01)00071-3

sheets so that the otherwise dominant glacio-isostatic contribution is relatively small.

In this paper we revise earlier estimates of sea-level and ice-volume change for the period prior to and leading into the LGM, starting at about 45,000 years ago, to the end of the major deglaciation about 7000 (calendar) years ago. Previous attempts have been made to infer ice volumes from sea-level observations for the period from the LGM to the present, most recently by Fleming et al. (1998). In some of the earlier solutions some systematic discrepancies between estimates of ice-volume-equivalent sea level have been identified when different observational data sets have been. Possibly they are artifacts of the interpretation of the observational evidence; that, for example, the growth positions of the corals occurred closer or further from mean sea level than assumed. Possibly they are a consequence of a tectonic contribution to the relative sea level change that has been inadequately corrected for. Possibly they are a consequence of inadequately modelled isostatic corrections or the use of unrepresentative values for some of the isostatic-model parameters. These issues are also explored in this paper.

2. Definition of ice-volume-equivalent sea level

The sea-level equation for a tectonically stable area may be written schematically as

$$\Delta\zeta_{\mathrm{rsl}}(\varphi,\, t) = \Delta\zeta_{\mathrm{e}}(t) + \Delta\zeta_{\mathrm{i}}(\varphi,\, t) + \Delta\zeta_{\mathrm{w}}(\varphi,\, t), \tag{1}$$

where $\Delta\zeta_{\mathrm{rsl}}(\varphi,\, t)$, the height of the palaeo sea surface relative to present sea level, is a function of position φ and time t. $\Delta\zeta_{\mathrm{e}}(t)$ is the "ice-volume-equivalent sea-level change" (defined by (3), below), or simply the equivalent sea-level change, associated with the change in ocean volume resulting from the melting or growth of land-based ice sheets.[1] $\Delta\zeta_{\mathrm{i}}$ and $\Delta\zeta_{\mathrm{w}}$ are the glacio- and hydro-isostatic contributions to sea-level change from the isostatic crustal displacement and associated planetary gravity-field or geoid change. Both $\Delta\zeta_{\mathrm{i}}$ and $\Delta\zeta_{\mathrm{w}}$ are functions of position and time. In formulating these terms ocean-ice mass is conserved and the ocean surface remains a gravitational equipotential surface throughout. The two load terms $\Delta\zeta_{\mathrm{i}}(\varphi,\, t)$ and $\Delta\zeta_{\mathrm{w}}(\varphi,\, t)$ are not wholly decoupled as implied by Eq. (1) and the interactions between the two are included in the actual formulation. The water depth or terrain elevation at time t at any location φ expressed relative to coeval sea level, is

$$h(\varphi,\, t) = h(\varphi,\, t_0) - \Delta\zeta_{\mathrm{rsl}}(\varphi,\, t), \tag{2}$$

where $h(\varphi,\, t_0)$ is the present-day (t_0) bathymetry or topography at φ. Both isostatic terms in (1) are functions of the earth rheology. The glacio-isostatic function is also a function of the ice mass through time and the hydro-isostatic function is a function of the spatial and temporal distribution of the water load: of the relative sea-level variation and of the migration of shorelines. The full solution of (1) therefore requires iteration with (2).

The term $\Delta\zeta_{\mathrm{e}}(t)$ relates to the total change in land-based ice volume V_{i} according to

$$\Delta\zeta_{\mathrm{e}}\,(t) = -\frac{\rho_{\mathrm{i}}}{\rho_{\mathrm{o}}}\int_{\mathrm{t}} \frac{1}{A_{\mathrm{o}}(t)}\frac{\mathrm{d}V_{\mathrm{i}}}{\mathrm{d}t}\,\mathrm{d}t, \tag{3}$$

where $A_{\mathrm{o}}(t)$ is the ocean surface area and ρ_{i}, ρ_{o} are the average densities of ice and ocean water, respectively. The ocean surface area is a function of time because of the advance or retreat of shorelines as the relative position of land and sea is modified and because of the retreat or advance of grounded ice over shallow continental shelves and seas. (That is, the ocean boundary is defined by the ice grounding-line and the ice volume includes grounded ice below coeval sea level.) The first dependence is a function of earth rheology and ice-load geometry which together determine the local rate of sea-level change. The second time dependence is a function of the location of the ice limits and whether the ice sheets are located above or below coeval sea level. Hence the relationship between ice volume V_{i} and equivalent sea level $\Delta\zeta_{\mathrm{e}}$ is model dependent and is determined iteratively along with the solutions of (1) and (2).

The theory underpinning the rebound and sea-level predictions has been well-developed since the important work of Peltier (1974), Cathles (1975) and Farrell and Clark (1976). Successive solutions of the sea-level equation have resulted in increased levels of sophistication and resolution (e.g. Nakada and Lambeck, 1987; Mitrovica and Peltier, 1991; Johnston, 1993, 1995; Milne and Mitrovica, 1998; Milne et al. 1999, for various aspects of the solution of the sea-level equation). While proper benchmarking has not yet been achieved, some comparisons between independent solutions have yielded consistent results at various stages of the model predictions. Thus three independent numerical solutions of the sea-level equation by Nakiboglu et al. (1983), Nakada and Lambeck (1987) and Johnston (1993, 1995) at ANU, for example, have yielded results whose differences are consistent with the consequences of the added complexity and resolution introduced into each of

[1] In the absence of other factors contributing to sea-level change (thermal expansion, melting of mountain glaciers not included in the ice models, or changes in ground- and surface-water storage) $\Delta\zeta_{\mathrm{e}}(t)$ corresponds to eustatic sea level. In Lambeck et al. (2000) and Yokoyama et al. (2000a) an erroneous distinction was made between the ice-volume-equivalent sea level and eustatic sea level (Yokoyama et al., 2001b; Lambeck et al., 2001). This erroneous estimate of the mean sea level at no stage feeds back into the main part of the sea-level calculation where the correct estimate has been used and the relative sea level predictions are unaffected.

the new-generation models. The earth-response functions have also been independently checked against the independent formulation by G. Kaufmann and while the latter results are more robust for long loading cycles ($\sim 10^5$ years and longer) agreement for shorter intervals corresponding to OIS 1-3, was found to be satisfactory. Preliminary comparisons of the ANU code with that developed by J.X. Mitrovica and G.A. Milne as well as with independent code developed by M. Nakada also leads to compatible results for localities far from ice margins.

If both the ice distribution through time and the earth's response to loading are known, then the equivalent sea level, and ice volumes through (3), follow from observed relative sea levels $\Delta\zeta_{\mathrm{rsl}}^{\mathrm{obs}}$ according to

$$\Delta\zeta_{\mathrm{e}} = \Delta\zeta_{\mathrm{rsl}}^{\mathrm{obs}} - (\Delta\zeta_{\mathrm{i}} + \Delta\zeta_{\mathrm{w}}), \quad (4)$$

where the $\Delta\zeta_{\mathrm{i}}$ and $\Delta\zeta_{\mathrm{w}}$ are the model-dependent isostatic corrections. The variance for $\Delta\zeta_{\mathrm{e}}$ is the sum of the variances of the observed and predicted quantities, where the latter includes the effect of uncertainties in the earth- and ice-model parameters and is estimated from forward predictions of the corrections for a range of plausible model parameters. Where the observational accuracies are asymmetric about the estimate of mean sea level, the variance of the predicted quantity is added to the square of the upper and lower limit accuracy or range estimates of the observation. For sites far from the ice margins the isostatic terms represent 10–15% of the sea-level signal at the LGM and Lateglacial times. Thus, if the corrective terms can be evaluated with an accuracy of 10%, the resulting uncertainty introduced into $\Delta\zeta_{\mathrm{e}}$ is of the order 1–2 m and smaller than most observational sea-level uncertainties.

3. Observational data

The observational data for sea-level change comes from different localities with different tectonic histories, covering different time periods, and representing different limiting estimates of past sea level. To combine these data into a single ice-volume-equivalent sea-level function it is therefore necessary to consider:

- Time scale; all observational data are reduced to the calendar time scale using the Calib 4.0 program of Stuiver et al. (1998) and the polynomial calibration of Bard et al. (1998) for the older ages. Ice models and viscosities, also, are defined in the calendar time scale (Lambeck and Nakada, 1991).
- Mean sea level; all estimates of the limiting values of sea level are reduced to mean sea level taking into consideration the relationship between formation or growth position of the sea-level indicator and mean sea level.
- Vertical tectonic land movement; sites that have been subjected to tectonic uplift or subsidence are corrected for this using, in most instances, the position of the Last Interglacial (LIg) and/or the mid-Holocene shoreline as an indicator of tectonic displacement.
- Isostatic effects; the 'corrective' terms ($\Delta\zeta_{\mathrm{i}} + \Delta\zeta_{\mathrm{w}}$) in (4) are applied. These corrections can exceed the equivalent sea-level change when sites lie within the former ice margins. For sites far from these margins, however, the corrections for the LGM and lateglacial are typically 10–15% of the observed change and isostatic corrections accurate to 10–15% will mostly suffice (see below).

3.1. Barbados

The Barbados coral data of Fairbanks (1989) and Bard et al. (1990a, b, 1993) remains an important source of information for relative sea level change during the late stages of the LGM and the Lateglacial period. The total data set includes duplicate radiocarbon ages and the range of values obtained for the same sample is used as a measure of dating precision. Differences in ages for the duplicate samples mostly lie within the formal accuracies given by the dating laboratories employed. Where duplicate ages are available for a single sample the weighted mean is used. All ages have been corrected for reservoir and isotopic fractionation effects. Thermal ionisation mass spectrometry (TIMS) uranium-series ages, when available, are used in preference to the radiocarbon ages and where only the latter are available they have been calibrated using the above mentioned calibration scales.

The samples are from several closely spaced cores through different coral colonies and hence may not represent a continuous record of coral growth. The corals represent lower limits to the position of sea level at the time of growth, the actual sea level at this time occurring above this position by a minimum of the tidal amplitude. Most of the sampled corals are *Acropora palmata* that has a well defined growth range of typically 3–7 m below mean sea level for Caribbean reefs (Lighty et al., 1982). Thus the average growth position adopted for *A. palmata* is 5 ± 2.5 m below mean sea level and the observed depths have been decreased by this amount. For the four *Porites asteroides* coral species a larger depth range of 8 ± 4 m has been adopted although colonies of this species can presently occur at greater depths (Fairbanks, 1989).

The elevation of the LIg reef on Barbados ranges from 60 m above sea level to <24 m (Radtke et al., 1988, and more recent unpublished data). Onshore of the coral core site this reef occurs at about 35 m elevation and this is the value adopted here together with an age of 124 ± 5 ka for the interval when sea levels were close to the present-day value. At the time of the LIg sea levels

were globally about 4 m above present (Stirling et al., 1998). The uplift rate is therefore about 0.25 ± 0.09 mm/year. The uncertainty estimate includes the contribution from the age uncertainty and an uncertainty of ± 10 m for the present elevation of the LIg reef at the core site. This value for the uplift compares with 0.34 mm/year adopted by Fairbanks, a value that is the average of uplift rates at two different sections; Clermont Nose (~ 0.45 mm/year) and Christchurch (~ 0.25 mm/year). The core site is closer to the latter and we have adopted the reef elevation given by Radtke et al. (1988, and more recent unpublished data).

Fig. 1a illustrates the estimated change in local mean sea level. The variance estimates are based on the sum of the squares of the individual contributions to the error budget. The results do not include the Holocene data points from localities other than Barbados that are included in the Fairbanks (1989) sea-level curve and these are discussed separately below.

3.2. Other Caribbean and West Atlantic locations

Lighty et al. (1982) have compiled a useful data set for sea-level change that extends back to about 11 000 years ago. All age determinations are based on radiocarbon dating and they have been calibrated to the calendar time scale. Age uncertainties are based on the formal precision estimates for the radiocarbon ages and on the precision of the calibration. All material corresponds to *A. palmata* and the same growth range as for the Barbados corals has been adopted. The localities contributing to the sea-level data before about 7000 years ago are assumed to have been tectonically stable over the last 11 000 years. The localities lie as far apart as Florida, Panama and Martinique but only the first two and St Croix include records older than about 7000 years. Significant differential isostatic effects can be anticipated between these sites (see below) such that this data should not be combined into a single relative sea-level curve. Fig. 1b summarizes the local relative sea-level results for the three localities.

In the final analysis only the Florida data is considered because it is the most complete and longest of the records and because, being closer to the Laurentide ice sheet than any of the other sites, it is useful as an indicator of the importance of this ice sheet on the isostatic predictions for Caribbean sites.

3.3. Tahiti

The data from Tahiti is from two drill cores (P6, P7) from an offshore site near Papeete harbour. The data is from Bard et al. (1996), with supporting information on coral species given by Montaggioni et al. (1997). Uranium series ages are used where available and where only radiocarbon ages are available the appropriate calibration has been applied. Accuracy estimates of the latter include the uncertainty in the calibration. Following Montaggioni et al. (1997) the following coral growth positions have been adopted: 4 ± 2 m for the branching communities of *Acropora* gr. *robusta-danai*, *Pocillopora cf. verrucosa*, and *Hydrolithon onkodes* (APH), 10 ± 5 m for the *Acropora* (tabula) colonies, and 12 ± 8 m for the Porites (domal) colonies. The deepest assemblages in the P7 core, at depths of about 83 m, correspond to APH communities and a growth position of 4 ± 2 m has been adopted.

Tahiti can be expected to undergo a slow tectonic subsidence from the relaxation of the volcanic load stresses in the lithosphere and, to a lesser degree, from the thermal contraction of a cooling lithosphere. The volcanic load is relatively young ($\sim 10^6$ years) and the relaxation time for the oceanic lithosphere for this region may be of the order of $\sim 10^7$ years (Lambeck, 1981). This yields a subsidence rate of about 0.1 mm/year or only about 1 m over 10 000 years. This is the value adopted here with an uncertainty of 50%. Bard et al. assumed a subsidence of 0.2 mm/year, based in part on an estimate of 0.15 mm/year by Pirazzoli and Montaggioni (1986, 1988) inferred from the elevations of mid-Holocene sea levels in the Society Islands. Differential sea-level change across the Society and Tuamotu island groups resulting from the isostatic effects, if neglected, can result in apparent relative tectonic signals of the order of 0.1 mm/year (Nakada and Lambeck, 1989) and the Pirazzoli and Montaggioni estimate may, therefore, be too high. Also, the value of 0.2 mm/year places the LIg surface at about 25 m below present sea level so that the actual location of this surface would provide a good constraint on the rate. Fig. 1c summarises the results for the local relative sea-level curve.

3.4. Huon Peninsula, Papua New Guinea

The Huon Peninsula is a rapidly uplifting area such that any LGM reefs can be expected at a depth as shallow as 40–60 m below present sea level. One drill core has been obtained from the raised Holocene reef at Kwambu, about 2 km southeast of Sialum. The data is from Chappell and Polach (1991). The samples have been radiocarbon dated using conventional methods. Edwards et al. (1993) have obtained uranium-series ages from samples in the same core and where these samples can be related to those of Chappell and Polach, the ages agree to within observational errors once the radiocarbon ages have been calibrated. Only the latter results are used, with accuracy estimates that include the calibration errors. The coral species dated include a mix of *Porites, Acropora, Montipora* and other species with *Porites* being dominant. All grow today in a considerable range of water depths along the Huon

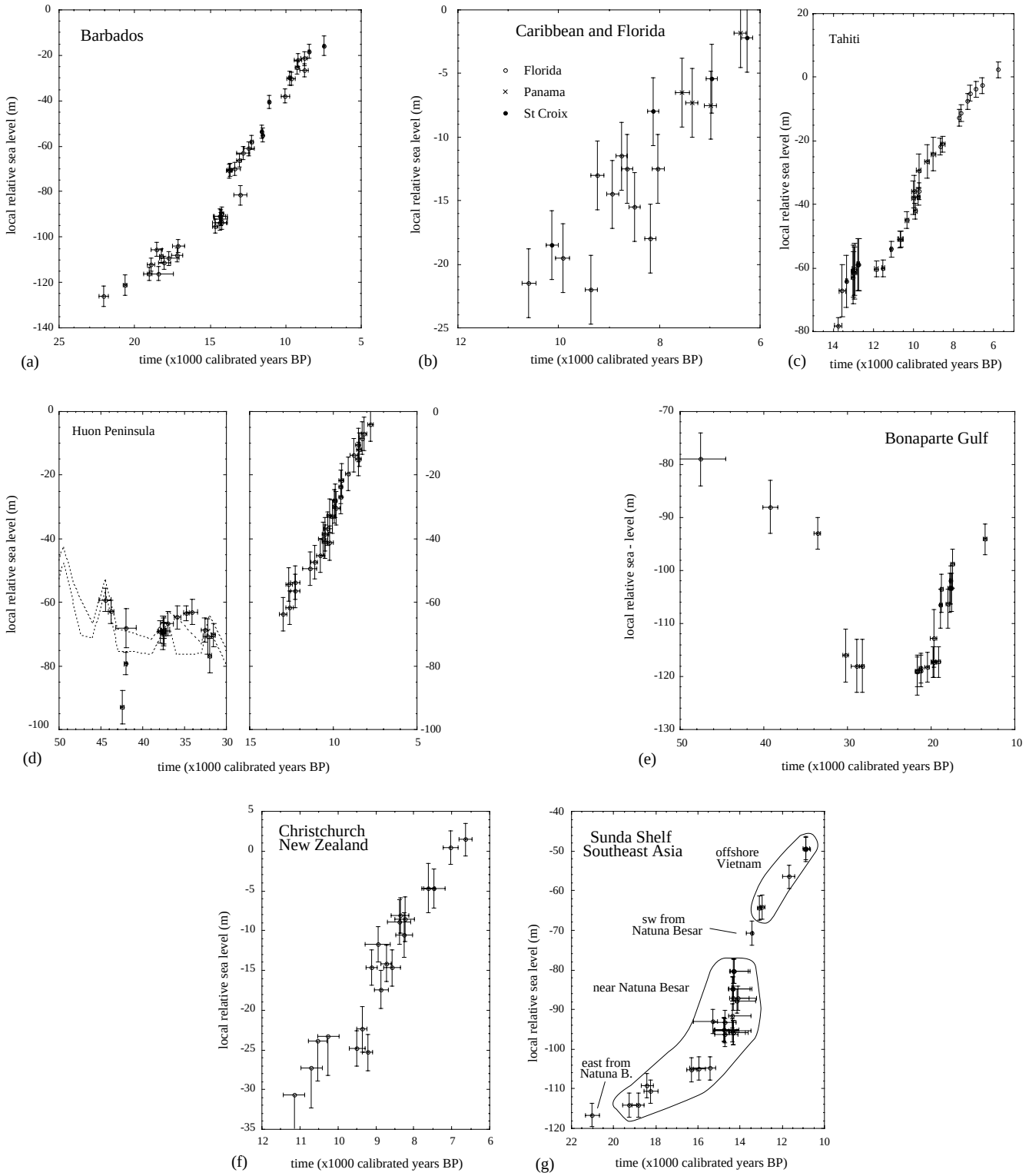

Fig. 1. Local relative sea-level functions inferred from observed shoreline height-age relationships. (a) Barbados, (b) two other Caribbean sites and Florida, (c) Tahiti, (d) Huon Peninsula, Papua New Guinea, for both the pre- and post-LGM periods, (e) Bonaparte Gulf, northwest Australia, including the pre-LGM evidence, (f) Christchurch, (g) Sunda Shelf, South East Asia. Note different scales used. In (b) and (g) results from locations with different isostatic corrections have been plotted on the same diagrams. In (d) the heights have been corrected for tectonic uplift and the sea-level uncertainties include contributions from uplift rates. The dashed line correspond to limits inferred from reef terrace morphology and facies analyses according to Chappell (2001).

coasts. The degree of detail about growth range available for Tahiti or the Caribbean is not available here and a range of 5 ± 5 m has been adopted for all corals.

All depths in the Kwambu core are given with respect to the top of the core which is at 6 m above mean sea level. The tidal amplitude is about 1 m. Kwambu is a region of rapid uplift with the LIg reef crest (reef VIIb) occurring at 227 m a.s.l., which suggests that the relative sea level early in the LIg interval was about 228 m above present level, compared to 2–4 m if there had been no tectonic uplift. This gives an average uplift rate of 1.76 ± 0.05 mm/year. The mid-Holocene reef crest at Kwambu occurs at 13 ± 1 m and has an age of 6800 ± 700 years (Chappell et al., 1996a) and mean sea level would have stood about 1 m above the reef flat. In the absence of tectonics this reef is expected to occur at 1.5 ± 0.5 m, based on models that have been calibrated against the Holocene data for the Australian margin (Lambeck and Nakada, 1990). Thus the average tectonic uplift for the past 7000 years has been 2.16 ± 0.44 mm/year, consistent with, but less precise than, the above longer-term average. The Huon reefs have now been studied in some detail along 40 km of coast and the uplift rates inferred from the LIg reef elevations vary from about 0.7 mm/year in the northwest to about 3.5 mm/year in the east. The mid-Holocene reef elevations are consistent with this regional late Quaternary trend and, when averaged over about 1000–2000 years, uplift rates at any one location estimated from either LIg or Holocene data are comparable (Chappell et al., 1996b). On shorter time scales, the uplift of the Huon peninsula is not uniform but occurs episodically, with a recurrence interval of 1000–1300 years and uplift magnitude of 1–2 m, both in the Holocene and late Pleistocene (Ota et al., 1993; Chappell et al., 1996b). Thus a co-seismic uplift component of $\sigma_s = 1.5$ m has been included in the above uncertainty estimates for sea level. Fig. 1d illustrates the results for the Lateglacial interval.

Because of the rapid uplift of the area any reefs formed before the LGM are mostly above present sea level and since the pioneering work of Chappell (1974) a number of attempts have been made to extract a sea-level record from the sequence of reefs (Chappell and Shackleton, 1986; Chappell et al., 1996a, b; Esat et al., 1999; Yokoyama et al., 2000b, 2001c). The early work has been variously hampered by inadequacies in the age determination of the corals, in the levelling of the reefs, and in the stratigraphic relationships of the coral growth position relative to coeval sea level. More recent surveys have rectified some of these deficiencies (Ota, 1994) and additional age determinations have been made by Omura et al. (1994) and Yokoyama (1999). All ages used below are based on uranium series dating methods, using both conventional alpha-counting and mass-spectrometric techniques. Standard acceptance criteria of all ages are used (Stirling et al., 1995, 1998). Where both methods have been used for the same sample the results agree to within the respective standard deviations of the age determinations. Also, duplicate ages in Chappell et al. (1996a) and Yokoyama (1999) agree, with one exception, to within their standard deviations. For the Chappell et al. (1996a) samples, information on the relationship of the coral growth position to sea level is available but for the other corals this information has to be inferred, either from nearby samples for which this information is available or by projecting the sampled coral position onto the nearest of the surveyed reef sections. Not all samples are from the same locality and local uplift rates have been established using the elevation of the LIg reef for each site. Fig. 1d summarizes the results for the Oxygen Isotope Stage (OIS) 3 interval.

One characteristic of the Huon reef data is that no reliable ages have been found younger than about 32 000 years for the later part of OIS-3. The fastest uplifting reefs occur at the Tewai River section with a rate of about 3.3–3.5 mm/year. Thus the absence of elevated reefs younger than this age indicates that sea levels during the remainder of OIS-3 did not rise above about 70–80 m below present-day levels.

3.5. Northwest Australia

The sea level information from the Northwest Shelf, Australia, has been discussed by Yokoyama et al. (2001a). It is from the shallow Bonaparte depression that was partly exposed at the time of the LGM with a central basin that was in open contact with the sea through several deep channels (van Andel et al., 1967). The information is obtained from cores whose sediment facies and fauna contain evidence for different water conditions at various times at locations that are now at different depths below present sea level. In particular a transition of conditions from open marine to shallow brackish-water environments has been identified in some of the cores corresponding to a late stage of the LGM. Only samples that are indicative of brackish or marginal marine conditions are used here. The former are believed to correspond to the tidal range within the broad depression and a formation depth of 2 ± 2 m has been adopted (Yokoyama et al., 2001a). Modern day equivalent of the marginal marine fauna correspond to water depths of less than 5 m and a formation depth of 4 m is adopted with upper and lower limits of 2 and 8 m, respectively. The accuracy estimates of the inferred local sea levels include depth and tidal amplitude uncertainties and the above uncertainties for the inferred water depth at time of deposition. Age estimates are based on calibrated AMS radiocarbon ages of foraminifera and, in a few cases, on conventional radiocarbon ages of

larger fauna. Reservoir corrections of 400 years have been applied.

The focus of the previous examination of the cores (Yokoyama et al., 2001a) was on the position of sea level during the LGM and the lower parts of the cores were not examined in the same detail once it was established that they corresponded to a period earlier than the termination of the maximum glaciation. Nevertheless, some useful results can be extracted for the pre-LGM period using the following guidelines. (i) Dates from the lowest part of a core are avoided because of the possibility of disturbance of the sediments during the coring; (ii) results are not used where reversals in age occur that exceed the accuracy of the AMS ages; (iii) the primary results are those where it has been possible to identify a sequence of facies change that enables the direction of sea-level change to be established; (iv) preference is given to results where several nearby horizons have been dated. Further analyses of the cores will be carried out for some of the critical transitions and the present results are therefore preliminary only. The results yielded eight acceptable sea-level indicators extending back to 47,000 (calendar) years.

The region of Northwestern Australia is assumed to be tectonically stable at the level of 0.1 m/ka. The LIg shoreline has not been identified along this section of the Australian coast, nor is the mid-Holocene highstand well defined here (e.g. Wright et al., 1972). However, conditions for preservation of shorelines within a few metres of mean sea level are not good in this region and the absence of these features is not necessarily an indication of subsidence. Results are summarized in Fig. 1e. The results are from different cores across the shelf and isostatic effects are important so it is not normally appropriate to plot all data onto a single curve without first correcting for the differential isostatic effects.

3.6. Christchurch, New Zealand

Evidence for sea level change extends back to about 11 000 years before present at the Banks Peninsula near Christchurch, South Island (Gibb, 1986). The record is from cored sediments that are indicative of mostly sheltered, low wave-energy palaeo estuarine and beach environments. The dated material includes estuarine intertidal molluscs in growth position using species that are common today and whose growth limits are known and are included in the associated accuracy estimates. Other samples include terrestrial peats and in situ tree stumps which give an upper limit to sea level of the highest astronomical tide or higher (sea levels are assumed to lie up to 4 m lower than these values in Fig. 1f). Reservoir corrections of 400 years have been applied to the mollusc data. All material has been radiocarbon dated using conventional methods and calibrated to the calendar time scale. The total accuracy estimates include measurement and calibration uncertainties.

A slow subsidence has been noted for the Banks peninsula and rates between 0.1 and 0.3 mm/year onshore and 0.05–0.09 mm/year offshore have been reported (see Gibb, 1986 for a summary). A value of 0.2 m/ka from Wellman (1979) has been adopted here with an uncertainty of 0.05 mm/year. The local sea level curve for this area is illustrated in Fig. 1f.

3.7. Sunda Shelf

An important recent data set is from the Sunda Shelf area, from a number of sediment cores between Vietnam, the Malay Peninsula and Kalimantan (Hanebuth et al., 2000). The importance of the record is that it extends from the LGM into the Holocene and that it fills in some of the Lateglacial gaps that occur in the coral record from Barbados. The cores sampled mangrove swamp, delta plains and tidal muds, lagoonal and other shoreline or near-shoreline facies from which the transgressive phase of sea-level rise has been identified. Radiocarbon dated materials include mangrove roots and other wood fragments, peaty detritus and plant residues and leach residues of bulk sediments. The ages in the deepest cores have been established mainly from the bulk sediment analyses and these results must be treated with some caution because of the possibility of contamination by older material. For example, Raymond and Bauer (2001) have shown that carbon input from river systems may lead to ages that are too old by as much as several thousand years (see also Chen and Pollach, 1986; Chichagova and Cherkinsky, 1993; Head and Zhou, 2000; Kretschmer et al., 2000). The calendar ages given by Hanebuth et al. are adopted as they used the same calibration functions as have been used above. Accuracy estimates of the inferred sea levels are difficult to assess from the available information because at a number of the sites it is not obvious that the dated material was in situ or had been transported at a later date. Thus all data points have been assumed to correspond to mean-sea-level with an uncertainty of ± 3 m.

The Sunda Shelf is believed to have been tectonically stable during the Pleistocene (Tjia and Liew, 1996) and no tectonic corrections have been applied. The offshore Vietnam site could be subject to some subsidence from the sediment load forming the Mekon Delta, but this is not considered here. Fig. 1g illustrates the results. Because of the wide spread of locations of the individual core sites it is almost certainly inappropriate to plot all data onto a single sea level curve without first correcting for any differential isostatic effects and this may well explain some of the apparent temporal variability seen in this figure (see below).

4. The rebound model

The theory used for predicting the isostatic corrections has been previously discussed and has been refined progressively (Nakiboglu et al., 1983; Nakada and Lambeck, 1987; Johnston, 1993, 1995; Lambeck and Johnston, 1998). The formulation used here for the Earth's response to loading has been tested against independent formulations and numerical codes (e.g. Kaufmann and Lambeck, 2000) and the sea-level predictions have been compared with observations for numerous areas around the world (Lambeck, 1993, 1995, 1996a, b, 1999; Lambeck et al., 1998, 2000). The parameters required to quantify the predictions describe the earth-response function and the surface-loading history. Once the ice load is defined as a function of position and time, the water load history is determined from knowledge of the ocean basin geometry, including the deformation of the basin through time, the migration of shorelines, and the retreat of ice across the shelves. The total ocean and ice mass is conserved and the ocean surface remains an equipotential surface at all times. Effects on sea level by changes in the gravitational attraction between the earth, ocean and ice as the load and planetary deformation evolves are included, as is the effect of glacially induced changes in earth rotation on sea level (Milne and Mitrovica, 1998).

For the earth response there may be no single set of rheological parameters that is appropriate for all regions because of the possibility of lateral variation in earth structure. For continental-margin Australia, for example, the upper-mantle viscosity appears to be less than it is for northern Europe (see Table 1). The sea-level change in the former region is primarily the result of the mantle response to water loading, with a flow of mantle material from beneath ocean lithosphere to beneath continental lithosphere. The resulting upper-mantle viscosity can, therefore, be considered as an average of ocean and continental mantle values. In contrast, the higher values from the Fennoscandian analyses reflect mainly the flow beneath the continental lithosphere. For only a few localities is there sufficient field evidence to enable regional response parameters to be estimated but, in a first approximation, the oceanic mantle viscosity can be expected to be less than that for continental mantle (Nakada and Lambeck, 1991; Lambeck, 2001). The effective viscosity beneath a continental margin is likely to lie between these values so that the mid-ocean mantle viscosity can be expected to be less than the viscosity beneath the Australian margin. Because of an absence of a full load-response formulation for lateral variability in mantle response, the isostatic corrections will be predicted here for a range of mantle parameters that embrace the values found for regions where mantle solutions have been possible (Table 1).

Table 1
Estimates for earth response parameters[a]

Model	H_l (km)	η_{um} ($\times 10^{20}$ Pa s)	η_{lm} ($\times 10^{22}$ Pa s)
Model values			
E0	65	4	1
E1	65	2	1
E2	65	6	1
E3	65	4	0.5
E4	65	4	3
E5	50	4	1
E6	80	4	1
E7	65	2	3
E8	65	1	1
E9	65	1	3
Values estimated from sea-level analyses			
Australia[b]	70–80	2–3	0.5–3
Australia[c]	75–90	1.5–2.5	(1)
Scandinavia[d]	65–85	3–4	0.6–1.3
British Isles[e]	65–70	4–5	0.7–1.3
Northwest Europe[f]	(65)	2-5	1–3
South Pacific[g]	~50	1	(1)

[a] Effective lithospheric thickness H_l and effective viscosities η_{um}, η_{lm} for the lower and upper mantle for different earth models used in predicting sea levels and inferred values from regional sea-level analyses.

[b] Lambeck and Nakada (1990), based on the analysis of the late Holocene data.

[c] Lambeck (2001), based on the analysis of the late Holocene data.

[d] Lambeck et al. (1998). The Scandinavian solution is from geological evidence since Lateglacial time.

[e] Lambeck et al. (1996). The British Isles solution is based on Lateglacial and Postglacial geological data.

[f] Kaufmann and Lambeck (2000). This solution is based on sea level and global rotational constraints, the latter constraining primarily the lower mantle [the values correspond to depth-averaged values and the lithospheric thickness was assumed known and equal to that determined in footnote d].

[g] Nakada and Lambeck (1991). The South Pacific result is a preliminary solution in which the lower mantle estimate is assumed known.

4.1. Regional variability

The far-field sea-level changes produced by the glacio-hydro-isostatic process are spatially variable mainly because of the different water loading effects at different sites. Thus it will not usually be valid to combine observed values from different locations into a single sea-level curve. Figs. 2 and 3 illustrate some examples of the predicted regional variability for the nominal earth model E0 (Table 1). The ice model I0 includes ice over North America, Europe and Antarctica with a total ice volume that is compatible with an earlier estimate of the ice-volume-equivalent sea level (Fleming et al., 1998) and in which the LGM is of relatively short duration, about 5000 years.

For the Bonaparte Gulf the cores are taken at different distances from the present coast: GC9 is

nearest to the shore and some 120 km from it, GC5 is in the middle of the depression and a further 120 km seaward, and V229 is near the edge of the shelf.

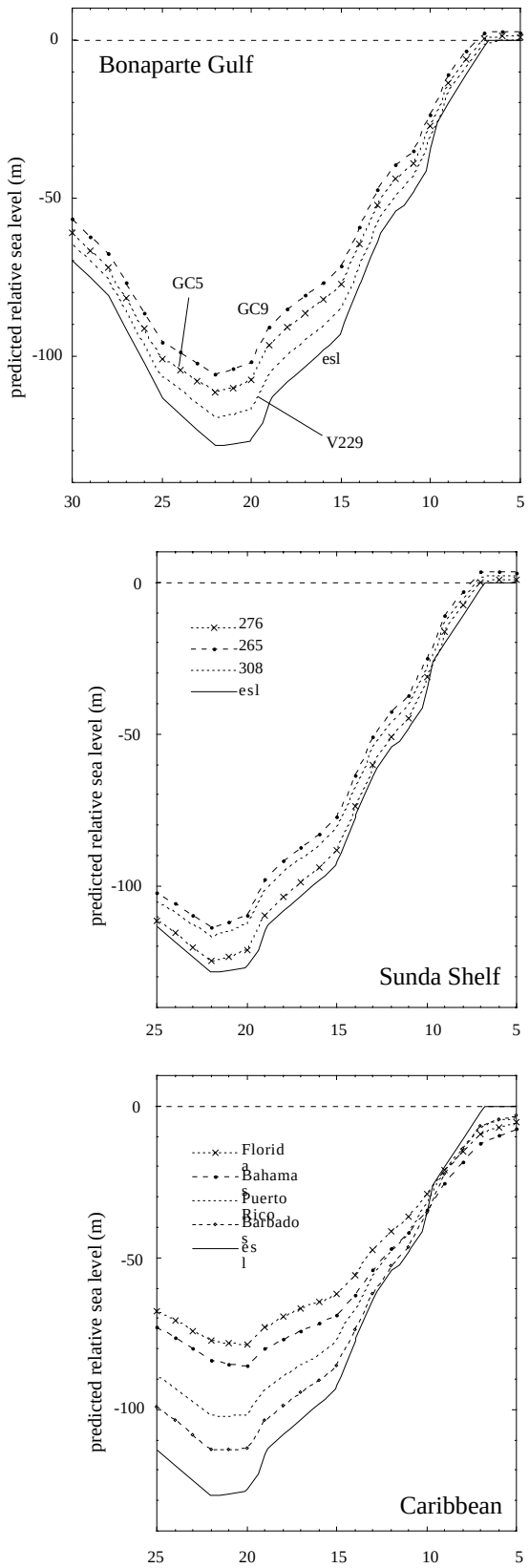

Differences between the three predictions are substantially larger than the precision of the sea-level observations and in this case the data from the different cores should not be combined into a single sea-level curve without first correcting for differential isostatic effects. Note that for all three sites the predicted sea levels lie above the corresponding ice-volume-equivalent sea-level function. The second example is for the Sunda Shelf sites where the core locations lie up to 800 km apart. Core (18)265 is offshore Vietnam, core (18)308 is near Natuna Besar and core (18)276 is some 180 km to the east of Natuna Besar and some 300 km from the Kalimantan coast. Fig. 3 illustrates the spatial variability predicted across the region for three epochs and demonstrates the importance of the water loading contributions, the differences reaching 20 m at the time of the LGM. Even between the core sites clustering near Natuna Besar the spatial variability is not unimportant and these data points should not be combined into a local sea level curve without first correcting for these differences. The third example in Fig. 2 is from the Caribbean, including Florida. Here there is a major north-south systematic progression in the shape of the predicted sea-level curve because of the glacio-isostatic rebound of the Laurentian ice sheet. Even at Barbados this glacio-isostatic effect is not negligible, as can be seen by the shape of the curve for the Late Holocene at which time the predicted sea levels are still rising and the mid-Holocene highstands that are characteristic of more distant sites are not seen here. The predicted differences between sites are substantial and the sea-level observations of Lighty et al. (1982) should not be combined with the Barbados data without first correcting for differential isostatic effects.

4.2. Earth-model dependence

While far-field Lateglacial sea-level predictions often are not strongly earth-model dependent (Lambeck and Nakada, 1990), this is not necessarily so for the time of the LGM. Fig. 4 illustrates a series of predictions of the

Fig. 2. Predicted relative sea levels for three regions illustrating the spatial variability within each region resulting from the glacio-hydro-isostatic effects. The predictions for the Bonaparte Gulf correspond to three cores (GC5, GC9, V229) at increasing distance from the present coast line. The curve identified as esl corresponds to the ice-volume-equivalent sea-level function. The predictions for the Sunda Shelf correspond to offshore Vietnam (core (18)265), a site well east of Natuna Besar (core (18)276) and to the main group of cores (core (18)308) (within this latter group significant variation in the isostatic effect still occurs because the coastline geometry here results in steep spatial gradients of the hydro-isostatic contribution, see Fig. 3 below). The spatial variability at these two sites is mainly the result of the hydro-isostatic contribution. The Caribbean results illustrate the strong gradient in the isostatic effect across the region due primarily to the glacio-isostatic contribution from the Laurentide ice sheet.

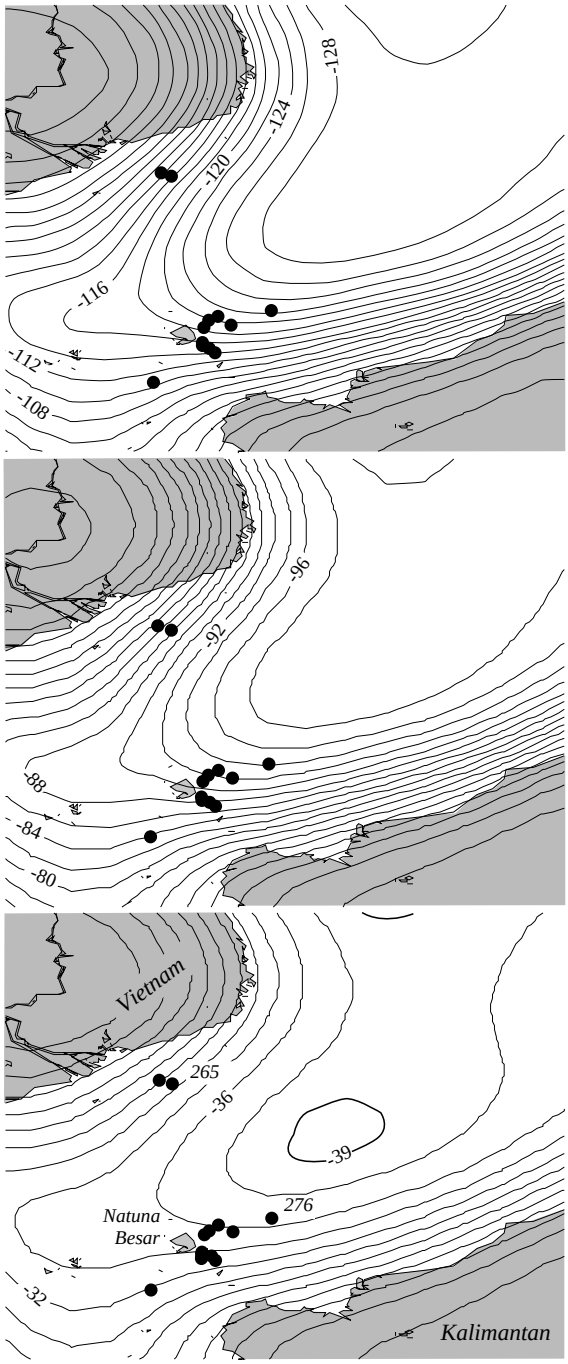

Fig. 3. Predicted spatial variability of sea level across the Sunda Shelf at three epochs (20, 15 and 10 ka, respectively). The solid circles indicate the core sites from Hanebuth et al. (2000). The predictions are for the nominal model parameters E0 and I0. Contour intervals are at 2 m.

isostatic corrections (rotation terms are not included in these examples) at three sites for the range of earth models defined in Table 1. For the island site of Tahiti the principal dependence is on mantle viscosity with lower values for either upper (E1) or lower mantle (E3) viscosities resulting in larger isostatic corrections in Lateglacial times. For Barbados, the principal dependence is on lower-mantle viscosity (compare E3 and E4), with, in this case, the higher value (E4) leading to larger isostatic corrections for the Lateglacial interval. The different behaviour of the isostatic term for these two sites reflects the greater role played by the glacio-isostatic term (primarily from the Laurentide rebound) for Barbados than for Tahiti. For Huon, the dependence is similar to that for Tahiti. The *differences* in the amplitudes of the corrections for the model range considered is about 6 m at the LGM for all three sites. For Christchurch (New Zealand), this difference reaches nearly 10 m at the LGM because of the relative close proximity of the Antarctic ice. For Florida it is 5–7 m for early to middle Holocene time, about twice that for Barbados at the same time.

4.3. Ice-model dependence

Fig. 5 illustrates the ice model dependence of the isostatic corrections for some of the sites. For the North American ice sheet two models have been considered, with similar ice-volume-equivalent sea-level values at the end of the LGM but the melting of one (I1) leading that of the nominal model (I0) by between 2000 and 3000 years during the Lateglacial interval. Other ice sheets have remained unchanged and the two ice-volume-equivalent sea-level functions (I0, I1) for the total change in ice volume are illustrated in Fig. 5a. Differences in the predicted isostatic corrections for the two models are illustrated in Fig. 5b. With the exception of Florida, these differences are $< \pm 3$ m whereas for Florida they exceed 10 m, reflecting the strong input from the North American ice sheet. The dependence of the isostatic corrections on the Antarctic ice model is illustrated in Fig. 5c for the model I2. In this case the Antarctic melting is assumed to lag that of the standard model (I0) such that the total function lags by about 1000 years. Differences in predicted isostatic corrections for these two ice models do not exceed 3 m for the far-field sites considered here. Thus sea level at these distant sites is sensitive to the total volume of meltwater contained in the ice sheets but, with the exception of Florida, insensitive to the distribution of this meltwater between the ice sheets.

4.4. Dependence on pre-OIS 2 sea levels

The observational evidence from both Huon and Bonaparte Gulf extend back in time to about 50,000 years, including the interval leading into the LGM. To predict the isostatic corrections for this earlier period the ice models need to be extended back to at least the LIg period. The Huon reefs provide the necessary information to about 140 000 years ago (Chappell, 1974; Chappell and Shackleton, 1986; Omura et al., 1994; Esat et al., 1999; Lambeck and Chappell, 2001;

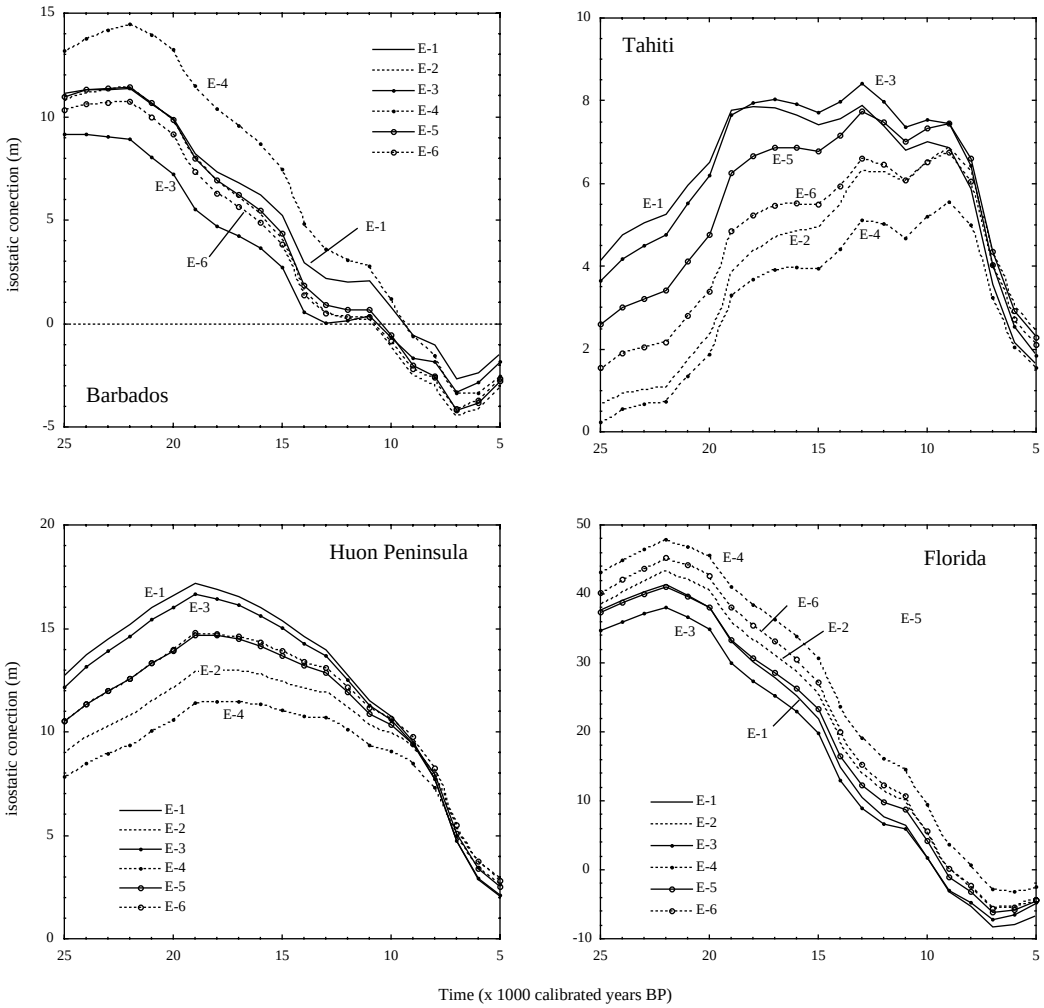

Fig. 4. Earth-model dependence of the isostatic corrections ($\Delta\zeta_i + \Delta\zeta_w$) for the six models E1–E6 defined in Table 1 which encompass the range of likely effective parameters for three-layered mantle models. Models E1 and E2 differ in upper-mantle viscosity with $\eta_{um}(E2) > \eta_{um}(E1)$. Models E3 and E4 differ in lower-mantle viscosity with $\eta_{um}(E4) > \eta_{um}(E3)$. Models E5 and E6 differ in lithospheric thickness with $H_l(E6) > H_l(E5)$.

Yokoyama et al., 2000b, 2001c; Chappell, 2001). All reef-elevation and age data, including low-stand information, has been re-evaluated and a number of inconsistencies between the various data sets have been identified and in most instances resolved through a re-examination of the original field notes held at ANU. As illustrated in Figs. 4 and 5 the LGM isostatic contributions are not negligible for the Huon Peninsula but are mainly a function of the sea-level rise and fall itself. This will also be the case for the earlier interval and thus a first-order pre-LGM ice sheet has been constructed with the assumption that when sea level before the LGM equals sea level at some time during or after the LGM the ice distributions for the two epochs are the same. Fig. 6 illustrates the resulting estimates for the ice-volume-equivalent sea levels for the past 140 000 years, based on the Huon and Bonaparte data. The sea-level fall leading up to the OIS-6 glacial maximum is assumed to have occurred linearly over a period of 90 000 years. Because predictions of the isostatic corrections during the latter part of the last glacial cycle (OIS-3) are insensitive to the details of this early part of the ice history, this simplification introduces negligible errors for the period of interest.

One feature of the pre-LGM record is that the maximum glaciation may have persisted for about 10,000 years (see Fig. 1) whereas the ice models discussed so far have assumed a much shorter duration (cf. Fig. 2a). The extended LGM model is based on a few data points from Bonaparte Gulf and on an absence of raised reefs younger than about 32,000 years from the most rapidly uplifting reef sections of Papua New Guinea. Any uncertainty in this duration will influence the isostatic predictions for the LGM and Lateglacial interval. Fig. 7 illustrates the predicted sea levels for two models, I0 and I3. The I3 model (Fig. 7a) represents a limiting case in which the LGM ice volumes were reached a sufficiently long time ago for equilibrium

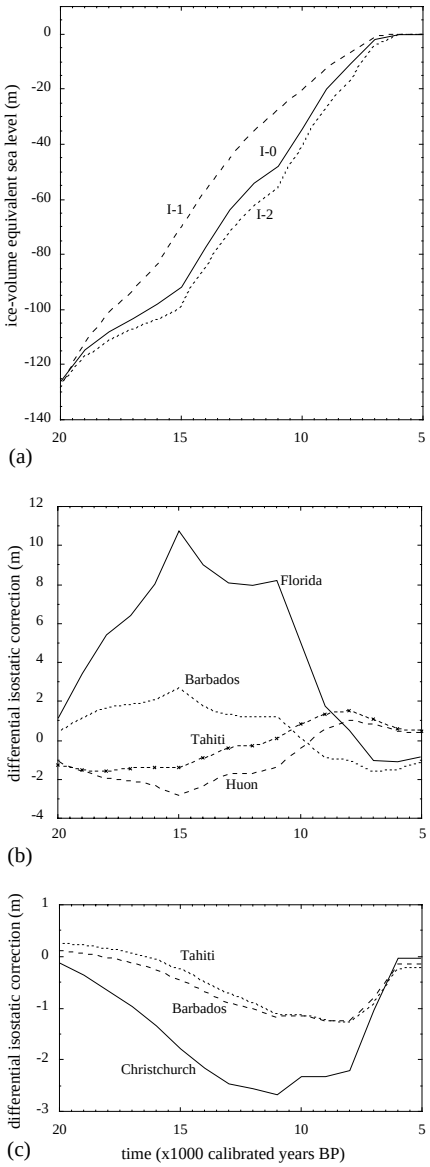

Fig. 5. Ice-model dependence of sea-level predictions at sites far from the former ice margins. (a) The ice-volume-equivalent sea-level function for three ice models: I0, the nominal ice model; I1, in which the northern hemisphere melting leads that of I0; I2, in which Antarctic melting lags behind that of I0. In all three models melting has ceased at 7000 calendar years ago. (b) The differential sea-level predictions for the nominal earth model E0 and the two ice models I0 and I1. (The abrupt changes in the gradients of these functions are an artifact of the melting history of the ice sheets which is represented by piecewise linear functions resulting in concomitant changes in rates of the elastic response and gravitational attraction of the ice.) (c) The same as (b) but for the ice models I0 and I2.

conditions to have been reached before melting started. For Barbados the effect of the longer LGM duration is to lower the predicted relative sea level whereas for the Bonaparte Gulf the effect is to raise this level (compare Figs. 7b and c), the difference being the result of the different roles of the glacio- and hydro-isostatic contributions at the two sites. For both sites, and in particular for the Bonaparte Gulf, the correct choice for the pre-LGM ice model is of some importance and in the results discussed below the pre-LGM ice models inferred from the sea-level curve illustrated in Fig. 6 will be used.

4.5. Accuracy of rebound model predictions

The accuracy estimates for the predicted sea levels in Eq. (4) are estimated from the forward predictions based on a range of representative earth and ice models. For the earth model the variance estimates are based on the mean-square values of the differences of the models E1 to E6 in Table 1 from the standard model E0. For the ice model the quantity $\{(I1\text{-}I0)^2+(I2\text{-}I0)^2+(I3\text{-}I0)^2\}$ is used as estimate of the variance of ice-model uncertainty on the sea-level predictions. Fig. 8 illustrates the standard deviations for the two contributions as well as their combined effect. For most of the sites far from the former ice sheets these standard deviations do not exceed 4 m and are comparable to, or smaller than, the observational uncertainties. Of these sites, only for Florida do the accuracy estimates of the predicted sea levels become substantial, exceeding 10 m in Lateglacial times.

5. The ice-volume-equivalent sea-level function

The sea level estimates follow from (4) with the predictions based on the nominal earth (E0) and ice (I0) model parameters. Fig. 9 illustrates the results with the variances corresponding to (i) the variance of the (calendar) age determinations and (ii) the combined variance of the sea-level observation and prediction. These ice-volume-equivalent sea-level estimates are based on the 'continental-margin' earth model (E1) (dependence on lithospheric thickness is not strong for most of the sites considered, Fig. 3) and on the I2 ice model for the LGM and post-LGM ice distribution and whose pre-LGM ice distribution is derived from the ice-volume-equivalent sea-level function in Fig. 6. With the exception of the Florida results, the estimates for ice-volume-equivalent sea level are broadly consistent within the accuracy estimates. The result indicates a rapid rise in sea level from about 15 000–7000 years but any fine structure is masked within the scatter and error bars of the results for the different localities. Thus Fig. 9b illustrates the same results, but without the error bars, and some systematic discrepancies, other than for Florida, are now more obvious. In particular, the Barbados results, lie above the other estimates for the Lateglacial and early Holocene period whereas the Tahiti results for the Holocene part of the record tend to lie below the other estimates. These differences may be a result of (i) limitations of the model parameters used in the calculation of the isostatic corrections or (ii) the growth or formation depths of the various sea-level

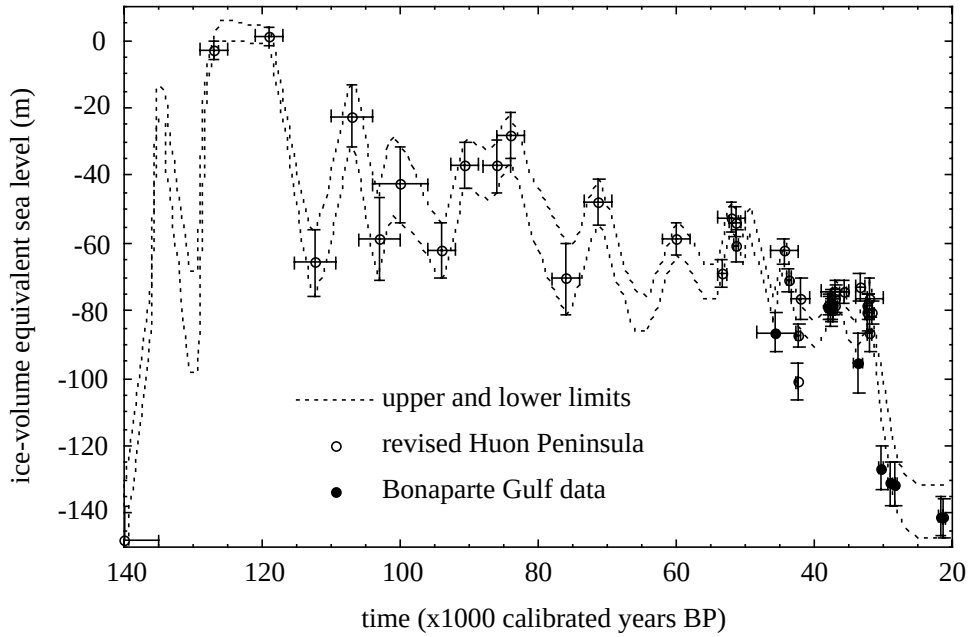

Fig. 6. Ice-volume-equivalent sea level for the last glacial cycle as inferred from the age-elevation relationship of raised coral reefs on the Huon Peninsula, Papua New Guinea and from sediments from the tectonically stable Bonaparte Gulf. The two dashed lines illustrate the upper and lower limits to the estimates.

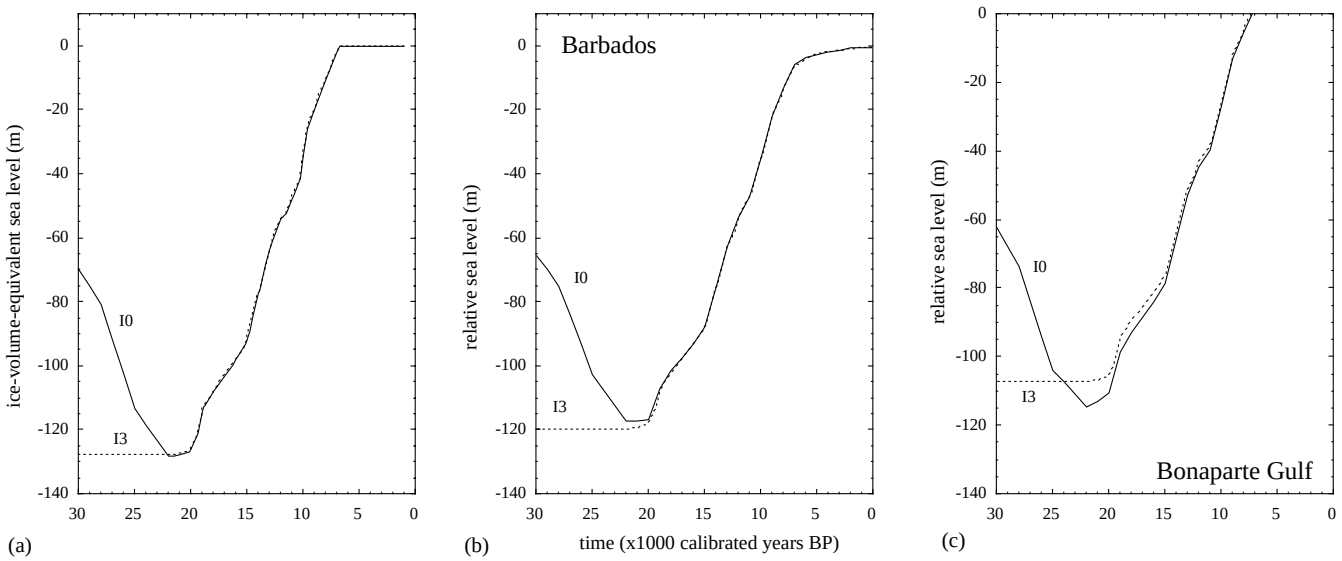

Fig. 7. Predicted sea levels for two ice models that differ in their duration of the LGM. In the nominal model I0 the LGM is of short duration whereas in model I3 LGM levels were reached an infinitely long time ago such that equilibrium conditions had been reached in the mantle before the onset of melting. (a) The ice-volume-equivalent sea-level functions for the two models; (b) predicted relative sea levels at Barbados, (c) predicted relative sea levels at Bonaparte Gulf (core GC-5).

indicators being systematically in error for some of the localities.

From Fig. 5, the only site for which the ice-volume-equivalent sea-level result is significantly dependent on details of the individual ice-sheet models is Florida, with the isostatic corrections for the two models I0 and I1 differing by 7–8 m at the time of the oldest data points. Model I1 for the North American ice sheet, for example, leads to shallower sea-level predictions for Holocene time and to increased ice-volume-equivalent sea-level estimates than does model I0 and, as illustrated in the inset of Fig. 9a, much of the previously noted discrepancy is reduced. For the other localities the inferred estimates based on these two ice models differ by no more than ± 2 m (see Fig. 5b) and the choice is not important.

Of the three rheological parameters that define the earth-response function, the least well determined is the effective lower-mantle viscosity. However, the far-field

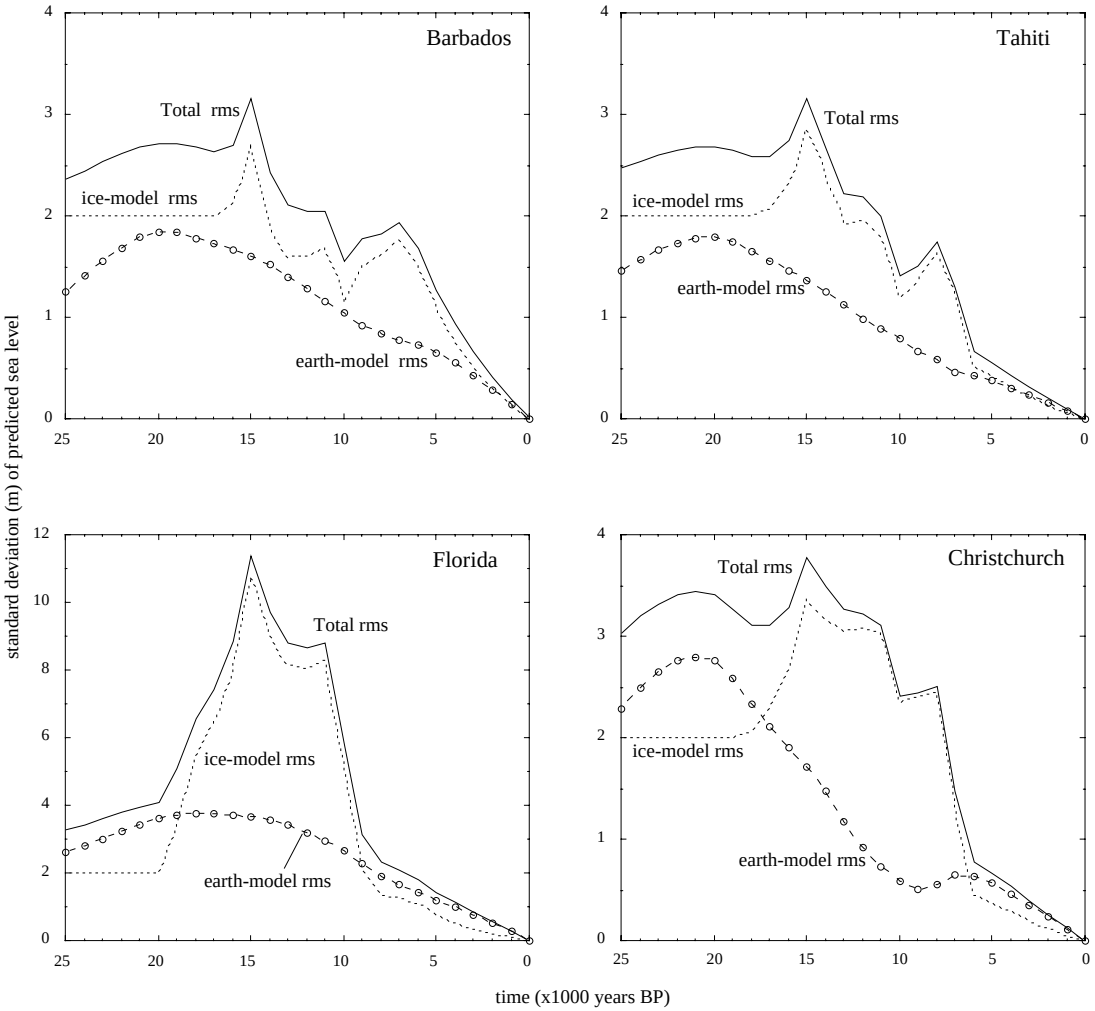

Fig. 8. Estimated standard deviations of the predicted isostatic corrections based on the nominal earth (E0) and ice (I0) models. The root-mean-square (rms) contributions from the earth-model and from the ice-model parameters are shown separately as well as the combined uncertainty estimate (total rms).

sites exhibit some dependence on this parameter (Fig. 4) because the response is mainly determined by the water load which has a long wavelength component that stresses the lower mantle more effectively than do the ice loads. From Fig. 4, increasing the lower-mantle viscosity (from model E3 to E4), increases the isostatic correction for both Barbados and Florida and lowers the inferred ice-volume-equivalent sea-level estimates for these sites. At Tahiti this relationship acts in the opposite direction, an increase in lower-mantle viscosity leading to a shallower estimate for the inferred ice-volume-equivalent sea level. The upper-mantle effective-viscosity of the nominal model E1 may also be inappropriate because any lateral variation in mantle response will result in lower estimates for this parameter for oceanic mantle. Lowering the upper-mantle viscosity for the Tahiti prediction, for example, increases the isostatic correction and lowers the resulting ice-volume-equivalent sea-level estimate. The same trend is predicted for Barbados. For Tahiti the consequences of an increase in lower-mantle viscosity and a decrease in upper-mantle viscosity tend to cancel out while for Barbados the effects of the two changes reinforce each other. In Fig. 10a the ice-volume-equivalent sea-level estimates for Barbados and Tahiti are based on the 'continental-margin' earth model (E1, Table 1), whereas the results in Fig. 10b are based on a model in which the lower-mantle viscosity is increased to 3×10^{22} Pa s (model E7, Table 1). In Fig. 10c it is the upper-mantle viscosity that has been reduced to 10^{20} Pa s (model E8, Table 1), to a value that may be representative of oceanic upper mantle. In both cases agreement between the two data sets is improved over that for the model E1. It should, therefore, be possible to find a set of rheological parameters, consistent with geophysical arguments and evidence for lateral variation, that leads to an optimum solution for the ice-volume-equivalent sea-level function in the sense of minimizing the differences between the individual records.

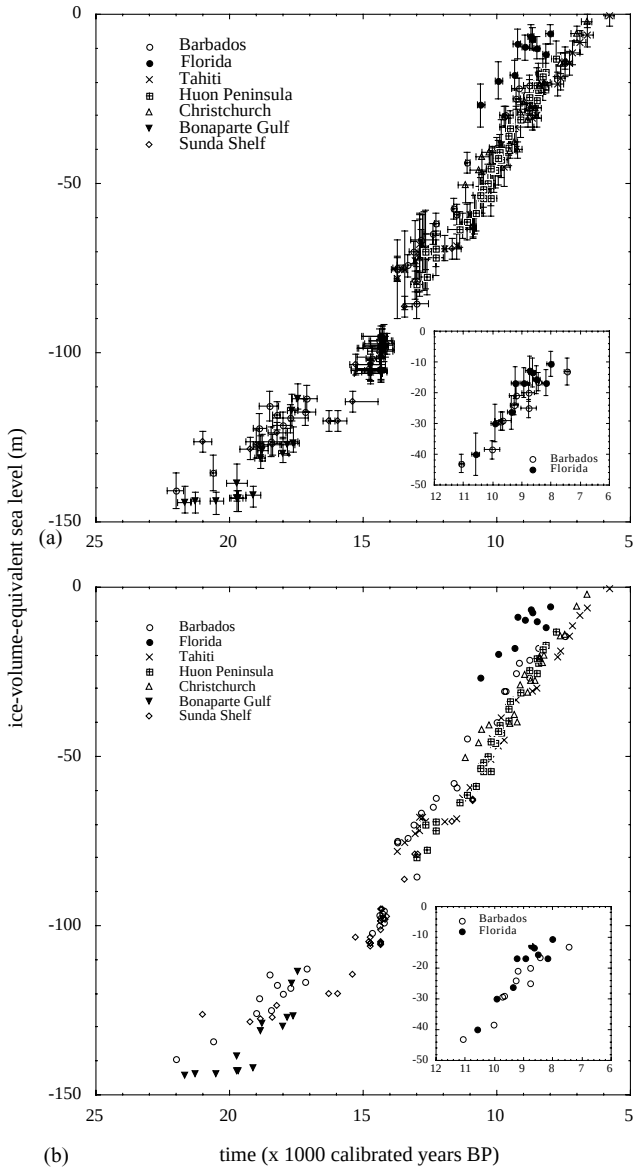

Fig. 9. Estimated ice-volume-equivalent sea-level estimates based on earth- and ice-model parameters (E1, I2 and the extended ice model corresponding to Fig. 6). (a) All data including the standard deviations of the estimates. The inset illustrates the results for Florida and Barbados based on the model parameters (E1, I1). (b) The same solution as (a) but without the standard deviations.

A formal inverse solution has not been attempted here, in part because some of the observational uncertainties are larger than the discrepancies seen in Fig. 9. However, the results from Fig. 10 indicate that earth models with a higher effective lower-mantle viscosity lead to a more consistent outcome and, in the final analysis, the model E7 is used for the continental-margin sites of Huon, Bonaparte, Sunda and Christchurch, and the model E9 (Table 1) is used for the ocean-island sites of Tahiti and Barbados. This choice of upper-mantle viscosity variation is consistent with preliminary solutions for lateral response (Nakada and Lambeck, 1991; Lambeck, 2001) while the increased

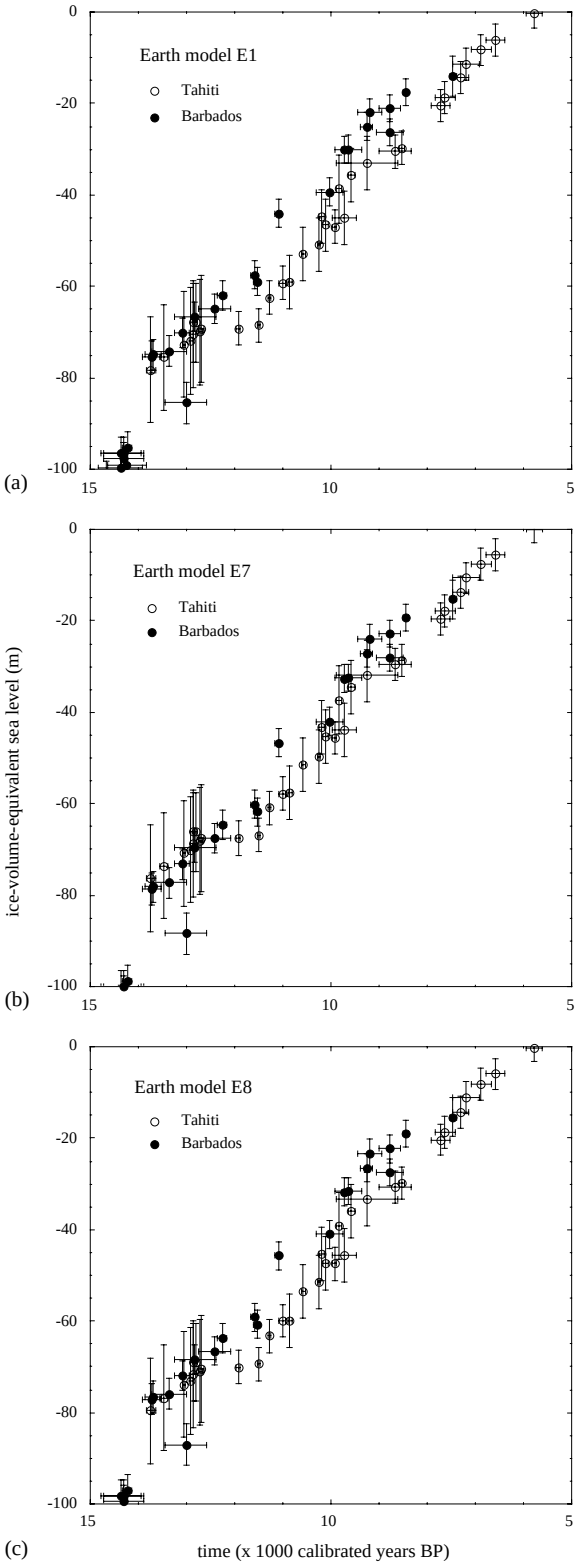

Fig. 10. Ice-volume-equivalent sea-level estimates for Barbados and Tahiti for different earth-model parameters (see Table 1) and the same ice model as for Fig. 9a. (a) Earth model E1, (b) earth model E7, (c) earth model E8.

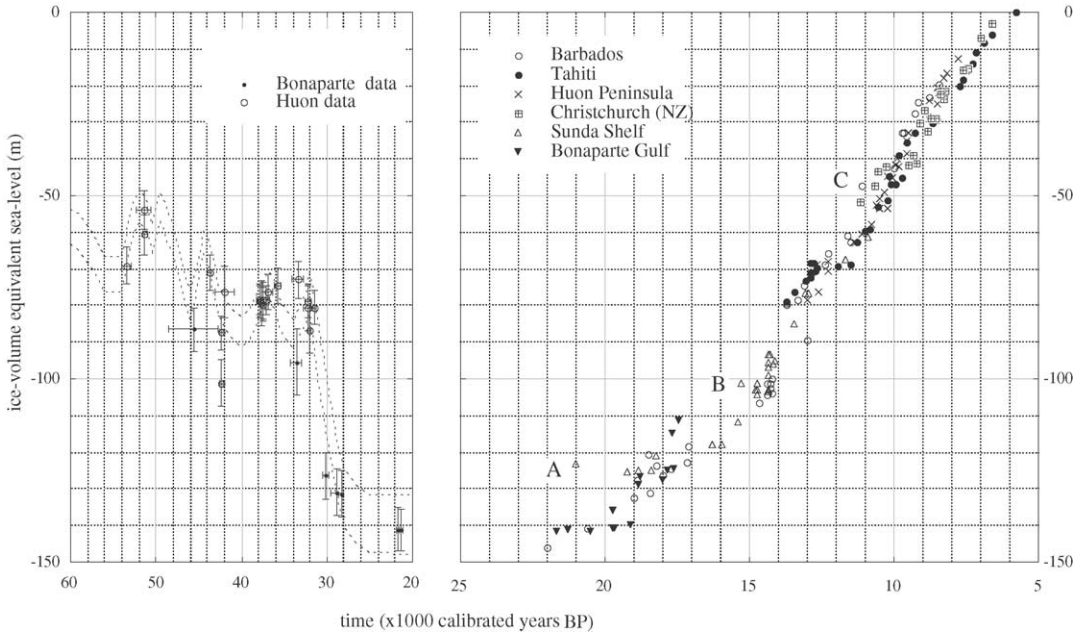

Fig. 11. Final solution for ice-volume-equivalent sea-level based on the continental-margin earth model E1 for the shelf sites (Huon Peninsula, Christchurch, Bonaparte Gulf, and Sunda Shelf) and the ocean earth model E9 for the mid-ocean sites (Barbados and Tahiti). The error bars for this solution are the same as in Fig. 9a.

lower-mantle viscosity is within the range of permissible solutions for this parameter (e.g. Kaufmann and Lambeck, 2000). Fig. 11 illustrates the results for the ice-volume-equivalent sea-level estimates for the LGM and post-LGM period as well as for OIS-3.

6. Discussion

6.1. End of the LGM and Lateglacial period

The results summarized in Fig. 11 refer to the mean estimates of ice-volume-equivalent sea level and the corresponding accuracy estimates are the same as those given in Fig. 9a. The results are indicative of a non-uniform increase in ocean volume, or decrease in grounded ice volume, from the time melting started at about 19 500 years BP. These changes can be characterized by several stages of different rates of sea-level change.

(i) Melting started at about 19,000 years ago and the initial rise may have been rapid, amounting to about 15 m in perhaps 500 years as discussed by Yokoyama et al. (2000a). The lowstand is defined by the Bonaparte and Barbados data where the growth depth of the Porites corals from the second data set has been assumed to be 8 ± 4 m. Only one Sunda Shelf data point at about 21,000 years ago (point A, Fig. 11) is inconsistent with the late LGM data. (This sample is one of the tidal flat bulk sediments whose ages may be contaminated by older carbon as suggested briefly above.)

(ii) Global melting was initially relatively slow with sea level rising from about 19 000–16 000 years BP at a rate of about 3.3 mm/year.

(iii) A more rapid and sustained rise occurred from about 16,000 to 12,500 years BP at an average rate of about 16.7 mm/year. (Note that the error bar of point B makes this point consistent with the cluster of points to its right.) The gap in the record at about 14,000 years BP could be construed as corresponding to a short duration very rapid rise but the Sunda data alone does not support this. This gap corresponds to the meltwater pulse 1A of Fairbanks (1989) and Bard et al. (1990a) (also referred to as 'catastropic rise event 1' by Blanchon and Shaw, 1995). Here we adopt the simpler interpretation of a linear rate for the entire interval.

(iv) A short-duration plateau in sea level rise may have occurred at about 12,500–11,500 years BP, corresponding to the time of the Younger Dryas. This has previously been noted by Edwards et al. (1993) and by Bard et al. (1996).

(v) The post Younger Dryas sea-level rise appears to have been rapid and uniform up to about 8500 years ago at a rate of about 15.2 mm/year. The combined data set does not indicate a particularly rapid sea-level rise (the meltwater pulse 1B of Fairbanks, 1989) following this plateau but the evidence is consistent with a prolonged uniform, but rapid, rising sea-level after the Younger Dryas. The Barbados data point at about 11,000 years ago (point C) appears to be inconsistent with the other

evidence at about this period, including the Christchurch (New Zealand) data which represent upper limits to the sea level.

(vi) By 7000 years ago ocean volumes approached their present-day level but did not attain it precisely until sometime later (Nakada and Lambeck, 1990; Lambeck, 2001)

6.2. OIS 3 and onset of the LGM

The Bonaparte data for this early interval needs further scrutiny but the results are consistent with the Huon reef data where the two data sets overlap in the late stage of OIS 3. The changes in sea level for this period can be characterized as follows.

(i) The LGM ice volumes were approached at about 30,000 years BP and increased only slowly during the next 10,000 years. We define the onset of the LGM as the time sea levels first approached their minimum levels at about 30,000 years ago.

(ii) The fall in sea level leading up to the LGM appears to have been rapid, about 50 m in less than 1000 years.

(iii) During the cold period leading up to the LGM, rapid oscillations in sea level, with magnitudes of tens of metres in time intervals of 1000 years or less, are superimposed on a gradually falling level, implying that ice sheets can decay and grow rapidly in glacial environments (Yokoyama et al., 2000b, 2001c; Chappell et al., 2001).

Acknowledgements

The authors thank Edouard Bard, John Chappell and Till Hanebuth for providing supplementary information about their sea-level data sets. They also thank Patrick De Deckker for his assistance with the interpretation of the palaeontological data from the Bonaparte Gulf.

The authors thank the referees, Edouard Bard, Bruce Bills and Jeanne Sauber, for their comments on the manuscript.

References

Bard, E., Hamelin, B., Fairbanks, R.G., Zindler, A., 1990a. Calibration of the ^{14}C timescale over the past 30,000 years using mass spectrometric U–Th ages from Barbados corals. Nature 345, 405–410.

Bard, E., Hamelin, B., Fairbanks, R.G., 1990b. U–Th ages obtained by mass spectrometry in corals from Barbados: sea level during the past 130,000 years. Nature 346, 456–458.

Bard, E., Arnold, M., Fairbanks, R.G., Hamelin, B., 1993. ^{230}Th–^{234}U and ^{14}C ages obtained by mass spectrometry on corals. Radiocarbon 35, 191–199.

Bard, E., Hamelin, B., Arnold, M., Montaggioni, L.F., Cabioch, G., Faure, G., Rougerie, F., 1996. Deglacial sea-level record from Tahiti corals and the timing of global meltwater discharge. Nature 382, 241–244.

Bard, E., Arnold, M., Hamelin, B., Tisnerat-Laborde, N., Cabioch, G., 1998. Radiocarbon calibration by means of mass spectrometric $^{230}Th/^{234}U$ and ^{14}C ages of corals. An updated data base including samples from Barbados Mururoa and Tahiti. Radiocarbon 40, 1085–1092.

Cathles, L.M., 1975. The Viscosity of the Earth's Mantle, Princeton University Press, Princeton, NJ, 386pp.

Chappell, J., 1974. Geology of coral terraces, Huon Peninsula, New Guinea: a study of quaternary tectonic movements and sea-level changes. Geological Society of American Bulletin 95, 553–570.

Chappell, J., 2001. Sea level changes triggered rapid climate shifts in the last glacial cycle: new results from coral terraces. Quaternary Science Reviews, in press.

Chappell, J., Polach, H., 1991. Post-glacial sea-level rise from a coral record at Huon Peninsula, Papua New Guinea. Nature 349, 147–149.

Chappell, J., Shackleton, N.J., 1986. Oxygen isotopes and sea level. Nature 324, 137–140.

Chappell, J., Omura, A., Esat, T., McCulloch, M., Pandolfi, J., Ota, Y., Pillans, B., 1996a. Reconciliation of late Quaternary sea levels derived from coral terraces at Huon Peninsula with deep sea oxygen isotope records. Earth and Planetary Science Letters 141, 227–236.

Chappell, J., Ota, Y., Berryman, K., 1996b. Late Quaternary coseismic uplift history of Huon Peninsula, Papua New Guinea. Quaternary Science Review 15, 7–22.

Chen, Y., Pollach, H., 1986. Validity of ^{14}C ages of carbonates in sediments. Radiocarbon 28, 464–472.

Edwards, R.L., Beck, J.W., Burr, G.S., Donahue, D.J., Chappell, J.M.A., Bloom, A.L., Druffel, E.R.M., Taylor, F.W., 1993. A large drop in atmospheric $^{14}C/^{12}C$ and reduced melting in the Younger Dryas, documented with ^{230}Th ages of corals. Science 260, 962–968.

Esat, T.M., McCulloch, T., Chappell, J., Pillans, B., Omura, A., 1999. Rapid fluctuations in sea level recorded at Huon Peninsula during the penultimate deglaciation. Science 283, 197–201.

Fairbanks, R.G., 1989. A 17,000-year glacio-eustatic sea level record: influence of glacial melting dates on the Younger Dryas event and deep ocean circulation. Nature 342, 637–642.

Farrell, W.E., Clark, J.A., 1976. On postglacial sea level. Geophysical Journal 46, 79–116.

Fleming, K., Johnston, P., Zwartz, D., Yokoyama, Y., Lambeck, K., Chappell, J., 1998. Refining the eustatic sea-level curve since the Last Glacial Maximum using far- and intermediate-field sites. Earth and Planetary Science Letters 163, 327–342.

Gibb, J.G., 1986. A New Zealand regional Holocene eustatic sea level curve and its application for determination of vertical tectonic movements. Bulletin of the Royal Society of New Zealand 24, 377–395.

Hanebuth, T., Stattegger, K., Grootes, P.M., 2000. Rapid flooding of the Sunda Shelf: a late-glacial sea-level record. Science 288, 1033–1035.

Head, M.J., Zhou, W.J., 2000. Evaluation of NaOH teaching techniques to extract humic acids from paleools. Nuclear Instrument and Methods in Physical Research B 172, 434–439.

Johnston, P., 1993. The effect of spatially non-uniform water loads on the prediction of sea-level change. Geophysical Journal International 114, 615–634.

Johnston, P., 1995. The role of hydro-isostasy for Holocene sea-level changes in the British Isles. Marine Geology 124, 61–70.

Kaufmann, G., Lambeck, K., 2000. Mantle dynamics, postglacial rebound and the radial viscosity profile. Physics of the Earth and Planetary Interiors 121, 301–324.

Kretschmer, W., et al., 2000. ^{14}C dating of sediment samples. Nuclear Instrument and Methods in Physical Research B 172, 455–459.

Lambeck, K., 1981. Lithospheric response to volcanic loading in the Southern Cook Islands. Earth and Planetary Science Letters 55, 482–496.

Lambeck, K., 1993. Glacial rebound of the British Isles. II: a high resolution, high-precision model. Geophysical Journal International 115, 960–990.

Lambeck, K., 1995. Late Pleistocene and Holocene sea-level change in Greece and southwestern Turkey: a separation of eustatic, isostatic and tectonic contributions. Geophysical Journal International 122, 1022–1044.

Lambeck, K., 1996a. Limits on the areal extent of the Barents Sea ice sheet in Late Weischelian time. Palaeogeography Palaeoclimatology Palaeoecology 12, 41–51.

Lambeck, K., 1996b. Shoreline reconstructions for the Persian Gulf since the Lastglacial maximum. Earth and Planetary Science Letters 142, 43–57.

Lambeck, K., 1999. Shoreline displacements in southern-central Sweden and the evolution of the Baltic Sea since the last maximum glaciation. Journal of the Geological Society London 156, 465–486.

Lambeck, K., 2001. Sea-level change from mid-Holocene to recent time: an Australian example with global implications. In: Mitrovica, J.X., Vermeersen, B. (Eds.), Glacial Isostatic Adjustment and the Earth System. Geophysical Union, American, in press.

Lambeck, K., Chappell, J., 2001,. Sea-level change through the last glacial cycle. Science 292, 679–686.

Lambeck, K., Johnston, P., 1998. The viscosity of the mantle: evidence from analyses of glacial rebound phenomena. In: Jackson, I. (Ed.), The Earth's Mantle. Cambridge University Press, Cambridge, pp. 461–502.

Lambeck, K., Nakada, M., 1990. Late Pleistocene and Holocene sea-level change along the Australian Coast. Palaeogeography Palaeoclimatology Palaeoecology (Global and Planetary Change Section) 89, 143–176.

Lambeck, K., Nakada, M., 1991. Sea-level constraints. Nature 350, 115–116.

Lambeck, K., Johnston, P., Smither, C., Nakada, M., 1996. Glacial rebound of the British Isles—III. Constraints on mantle viscosity. Geophysical Journal International 125, 340–354.

Lambeck, K., Smither, C., Johnston, P., 1998. Sea-level change, glacial rebound and mantle viscosity for northern Europe. Geophysical Journal International 134, 102–144.

Lambeck, K., Yokoyama, Y., Johnston, P., Purcell, A., 2000. Global ice volumes at the last Glacial Maximum. Earth and Planetary Science Letters 181, 513–527.

Lambeck, K., Yokoyama, Y., Johnston, P., Purcell, A., 2001. Corrigendum to "Global ice volumes at the Last Glacial Maximum and early Lateglacial. Earth and Planetary Science letters 190, 275.

Lighty, R.G., Macintyre, I.G., Stuckenrath, R., 1982. *Acropora palmata* reef framework: a reliable indicator of sea level in the western Atlantic for the past 10,000 years. Coral Reefs 1, 125–130.

Milne, G.A., Mitrovica, J.X., 1998. Postglacial sea-level change on a rotating earth. Geophysical Journal International 133, 1–19.

Milne, G.A., Mitrovica, J.X., Davis, J.L., 1999. Near-Field Hydro-Isostasy: The Implementation of a Revised Sea-Level Equation. Geophysical Journal International 139, 464–482.

Mitrovica, J.X., Peltier, W.R., 1991. A complete formalism for the inversion of post-glacial rebound data: resolving power analysis. Geophysical Journal International 104, 267–288.

Montaggioni, L.F., Cabioch, G., Camoin, G., Bard, E., Ribaud-Laurenti, A., Faure, A., Dejardin, P., Recy, J., 1997. Continuous record of reef growth over the past 14 k.y. on the mid-Pacific island of Tahiti. Geology 25, 555–558.

Nakada, M., Lambeck, K., 1987. Glacial rebound and relative sea-level variations: a new appraisal. Geophysical Journal of the Royal astronomical Society 90, 171–224.

Nakada, M., Lambeck, K., 1989. Late Pleistocene and Holocene sea-level change in the Australian region and mantle rheology. Geophysical Journal International 96, 497–517.

Nakada, M., Lambeck, K., 1991. Late Pleistocene and Holocene sea-level change: evidence for lateral mantle viscosity structure? In: Sabadini, R., Lambeck, K., Boschi, E. (Eds.), Glacial Isotasy, Sea Level and Mantle Rheology. Kluwer Academic Publishers, Dordrecht, pp. 79–94.

Nakiboglu, S.M., Lambeck, K., Aharon, P., 1983. Postglacial sealevels in the Pacific: implications with respect to deglaciation regime and local tectonics. Ionophysics 91, 335–358.

Omura, A., Chappell, J.M.A., Bloom, A.L., 1994. Alpha-spectometric $^{230}Th/^{234}U$ dating of Pleistocene corals. In: Ota, Y. (Ed.), Study on Coral Reef Terraces of the Huon Peninsula. Papua New Guinea, Yokohama.

Ota, Y., 1994. Study on coral reef terraces of the Huon Peninsula, Papua New Guinea, Yokohama National University press, Yokohama, 171 p.

Ota, Y., Chappell, J., Kelley, R., Yonekura, N., Matsumoto, E., Nishimura, T., Head, J., 1993. Holocene coral reef terraces and coseismic uplift of Huon Peninsula, Papua New Guinea. Quaternary Research 40, 177–188.

Peltier, W.R., 1974. The impulse response of a Maxwell Earth. Review of Geophysics 12, 649–669.

Pirazzoli, P.A., Montaggioni, L.F., 1986. Late holocene sea-level changes in the northwest Tuamotu Islands, French Polynesia. Quaternary Research 25, 350–368.

Pirazzoli, P.A., Montaggioni, L.F., 1988. Holocene sea-level changes in French Polynesia. Palaeogeography Palaeoclimatology Palaeoecology 68, 153–175.

Radtke, U., Grün, R., Schwarcz, H.P., 1988. Electron spin resonance dating of the Pleistocene coral reef tracts of Barbados. Quaternary Research 29, 197–215.

Raymond, P.A., Bauer, J.E., 2001. Riverine export of aged terrestrial organic matter to the North Atlantic Ocean. Nature 409, 497–500.

Stirling, C.H., Esat, T.M., McCulloch, M.T., Lambeck, K., 1995. High-precision U-series dating of corals from western Australia and implications for the timing and duration of the last interglacial. Earth and Planetary Science Letters 135, 115–130.

Stirling, C.H., Esat, T.M., Lambeck, K., McCulloch, M.T., 1998. Timing and duration of the Last Interglacial: evidence for a restricted interval of widespread coral reef growth. Earth and Planetary Science Letters 160, 745–762.

Stuiver, M., Reimer, P.J., Bard, E., Beck, J.W., Burr, G.S., Hughen, K.A., Kromer, B., McCormac, G., Van der Plicht, J., Spurk, M., 1998. INTCAL98 radiocarbon age calibration, 24,000-0 cal BP. Radiocarbon 40, 1041–1083.

Tjia, H.D., Liew, K.K., 1996. In tectonic evolution of Southeast Asia. Geological Society Special Publication 291–.

van Andel, T.H., Heath, G.R., Moore, T.C., McGeary, D.F.R., 1967. Late Quaternary history, climate, and oceanography of the Timor Sea, northwestern Australia. American Journal of Science 265, 737–758.

Wellman, H.W., 1979. An uplift map of the South Island of New Zealand, and a model for uplift of the Southern Alps. Royal Society of New Zealand, Bulletin 18, 13–20.

Wright, L.D., Coleman, J.M., Thom, B.G., 1972. Emerged tidal flats in the Ord River estuary, Western Australia. Search 3, 339–341.

Yokoyama, Y., 1999. Sea-level change in Australasia and the Radiocarbon time scale calibration during the last 50,000 years. Ph.D. Thesis, ANU, Canberra.

Yokoyama, Y., Lambeck, K., De Deckker, P., Johnston, P., Fifield, L.K., 2000a. Timing of the Last Glacial maximum from observed sea-level minima. Nature 406, 713–716.

Yokoyama, Y., Esat, T.M., Lambeck, K., Fifield, L.K., 2000b. Last ice age millennial scale climate changes recorded in Huon Peninsula Corals. Radiocarbon 42, 383–401.

Yokoyama, Y., De Deckker, P., Lambeck, K., Johnston, P., Fifield, L.K., 2001a. Sea-level at the last glacial maximum: evidence from northwestern Australia to constrain ice volumes for oxygen isotope stage 2. Palaeogeography Palaeoclimatology Palaeoecology 165, 281–297.